RSC Advances

ROYAL SOCIETY OF CHEMISTRY

www.rsc.org/advances

Hydrophilic molecularly imprinted microspheres functionalized with amino and carboxyl groups for highly selective recognition of human hemoglobin in aqueous solution

Jia-Ping Lai [a], Yue Zuo [a], Hui Sun [b]*, Ying Yu [a]

Abstract: The hydrophilic molecularly imprinted microspheres (HMIMs) functionalized with amino and carboxyl groups have been synthesized successfully using human hemoglobin as template. The obtained HMIMs have been characterized with scanning electron microscope (SEM), adsorption isotherms, dynamic binding as well as quartz crystal microbalance (QCM). The rebinding results indicate that the HMIMs exhibit highly selective recognition property towards target human hemoglobin in Tris-HCl aqueous solution with an imprinting factor of 1.90 and a high binding capacity of 98 mg/g. The QCM characterization results also demonstrate that the HMIMs coated electrode shows a more sensitive response to hemoglobin than that of non-imprinted microspheres coated electrode.

Keyword: Hydrophilic molecularly imprinted microspheres, surface imprinting, quartz crystal microbalance, human hemoglobin

[a] School of Chemistry & Environment, South China Normal University, Guangzhou, 510006, China. E-mail: laijp@scnu.edu.cn; Fax: +86-20-39310187; Tel.: +86-20-39310257

[b] College of Environmental Science & Engineering, Guangzhou University, Guangzhou, 510006, China. E-mail: cherrysunhui@aliyun.com

1. Introduction

In recent decades, with the rapid development of post-genome era, the separation and enrichment of low abundance proteins play an important role in genomic research. Thus, it is urgent to explore highly efficient and selective materials for the separation and enrichment of those target proteins from complex samples. Molecularly imprinted polymers (MIPs) as biomimetic materials have attracted many researchers to pay attention because MIPs offer significant advantages such as high selectivity, good mechanical/chemical stability, reusability and low cost [1-8]. Thus, MIPs have been applied to various research fields such as medicine [5,9-11], food [12-16], environment [12, 14,17-21] and industry [22]. Recently, MIPs have been widely applied to recognize, analyze, separate and enrich various target proteins such as lysozyme [2,23-27], bovine hemoglobin [4,8], bovine serum albumin [7,28] and phycocyanin [29]. However, the large molecular size of protein shall cause a big problem for protein imprinting, because it restricts the mass transfer of proteins between the imprinted cavities and the solution [24, 29-31]. Other challenges for imprinting protein include the considerations on the flexible conformation, complex structure, and specific functional groups and so on. Up to now, a few imprinting approaches have been developed to solve the mass transfer problem of proteins such as surface imprinting [24,32-35], epitope imprinting [36-39] and

metal-coordination polymerization [25,40,41]. Among those, surface imprinting is a promising strategy to arrange the recognition sites on the surface of proper supporting material, such as silica microspheres, which makes it easier for the eluting and rebinding of target proteins [42,43].

On the other hand, the hydrophilicity of the surface of silica microspheres will have significant effect not only on the efficiently formation of binding sites during the imprinting process, but also on the access of hydrophilic protein from aqueous media to the imprinted material during the rebinding process. Since the hydrophilicity of the produced recognition material is critical to the sensitive detection for proteins [26, 31, 44], in this study, the surface of silica microspheres have been derivated to possess amino and carboxyl groups as the recognition functional groups to recognize the target proteins, and ploymerizable vinyl groups to produce the polymerizing interaction with functional monomer and crosslinker during the imprinting process. Finally, we successfully got the silica microspheres with hydrophilic surface and good recognition properties to human hemoglobin (HHb) in aqueous solution. The synthesis and characterization of the functionalized silica microspheres, as well as the hydrophilic HHb-imprinted microspheres shall be discussed in detail in the following.

2. Materials and methods

2.1 Chemicals and reagents

Silica microspheres (7~9 μm) were provided by local commercial suppliers. Toluene was purchased from Hunan Hengyang Kaixin Chemical Co., LTD and distilled before used. 3-Aminopropyl-trimethoxysilane (APTMS), N,N,N',N'-tetramethylethylenediamine (TEMED), 2-(dimethylamino)ethyl methacrylate (DMAEMA), lysozyme (Lys) and bovine serum albumin (BSA) were purchased from Aladdin Reagent Co., Ltd. Human hemoglobin (HHb) was purchased from Sigma-Aldrich Co., Ltd. Methacrylic acid (MAA) and acrylamide (AAm) were purchased from Tianjin Damao Reagents Co., Ltd. N,N'-methylenebisacrylamide (MBA) was purchased from Tianjin Chemical Reagents Co., Ltd. Ammonium per-sulfate (APS) was purchased from Tianjin Zhiyuan Reagents Co., Ltd. Tris(hydroxymethyl) aminomethane hydrochloride (Tris-HCl) was purchased from Sangon Biotech Bioengineering Co., Ltd. (Shanghai, China). All other chemicals were of analytical grade and used as received.

2.2 Synthesis and characterization of functionalized silica microspheres

The silica microspheres were mixed with HCl/H_2O(2:1,V/V) and refluxed at 60℃ for 12 h. Subsequently, the activated microspheres were washed with deionized water to neutral, and then treated according to the reported literature [43] with small modification (Scheme 1). Briefly, 1 g of silica microspheres was dispersed in 25 mL of anhydrous toluene after adding 1 mL of APTMS. The mixture reacted at 110℃ for 24 h under dry nitrogen to introduce amino group to the silica microspheres. Then, after washing with toluene and acetone repeatedly, the silica microspheres were dispersed in the mixture of N,N'-dimethylformamide (25 mL), maleic anhydride (1 g) and pyridine (2.5 mL), and reacted at 50℃ under dry nitrogen for 6 h. Finally, the functionalized microspheres were centrifugated and washed repeatedly with ethanol and deionized water for several times to remove unreactive reagents, and then dried under vacuum at 40℃ for the subsequent experiment. The functionalized microspheres were characterized with a FT-IR170 infrared spectrophotometer (Perkin Elmer, USA,) and a 2550 UV spectrophotometer (Shimadzu, Japan).

<Scheme 1>

2.3 Synthesis and characterization of the hydrophilic HHb-imprinted microphores

The HHb-imprinted microspheres were synthesized as described in scheme 1. The synthesis strategy was based on the protocol described in reference [26] with small modification. Concisely, in a 150-mL flask, MAA (76 μL, 0.916 mmol), DMAEMA (144 μL, 0.916 mmol), MBA (32 mg), and AAm (65.2 mg, 0.916 mmol) were mixed with 64 mL of Tris-HCl buffer (pH 7.0, 0.01M) by ultrasonic. At the same time, 16 mg of HHb was added into the mixture of 8 mL ethanol and 8 mL Tris-HCl buffer which has been dispersed with 240 mg of the functionalized microspheres (SiO_2-NH_2). And then the mixture was poured into the above flask, and purged with nitrogen for 10 min and agitated for 1h. Then 120 μL of TEMED solution (5%, w/v) and 240 μL of APS solution (10%, w/w) were injected to the flask. Finally, the polymerization was initiated and sustained with stirring at room temperature for 24 h. The HHb-imprinted microspheres were gathered by centrifugation. The microspheres obtained were washed with deionized water several times to remove the remained reactant. After that, they were washed with 0.5 M NaCl solution repeatedly to remove the template until no absorption signal of HHb could be detected at 406 nm in the supernatant using a Shimadzu UV-2550 UV spectrophotometer (Shimadzu, Japan). Then, they were washed with deionized water to remove residual NaCl and equilibrated with the Tris-HCl buffer (pH 7.0, 0.01M). Eventually, they were dried under vacuum at 25℃ to obtain the final hydrophilic HHb molecularly

imprinted microspheres (HMIMs). The control non-imprinted microspheres (NIMs) were prepared with the same method without adding the template HHb during polymerization. The morphology of the obtained HMIMs and NIMs was characterized by a JEOL JMS-7001F scanning electron microscopy (JEOL, Japan). The thermogravimetric analysis was carried using a STA409 PC thermo-gravimetric analyzer (Netzsch, German).

2.4 Adsorption experiments

The adsorption isotherms experiments were conducted as the following procedure: in a 25-mL conical flask, 20.0 mg of the prepared HMIMs and NIMs were suspended in 10 mL protein solution at a specific concentration in Tris-HCl buffer (pH 7.0, 0.01M), respectively. In adsorption experiment, the suspension was incubated with agitating for 12 h at room temperature. Then, after centrifugation at 3000 *g* for 5 min, the supernatant was determined by a Shimadzu UV-2550 UV spectrophotometer (Shimadzu, Japan) at 406 nm. The amount of protein adsorbed by the microspheres was calculated with the following formula:

$$Q = \frac{(C_{\mathrm{i}} - C_{\mathrm{f}})\,\mathrm{V}}{m}$$

where Q (mg g^{-1}) is the mass of protein adsorbed by unit mass of dry microspheres, C_{i} and C_{f} (mg mL^{-1}) are the concentrations of the initial

and final solutions respectively, V (mL) is the total volume of the adsorption mixture, *m* (mg) is the mass of the microspheres used.

The adsorption kinetics of the prepared microspheres was investigated with HHb solution with concentration of 0.2 mg mL^{-1}. The protocol of adsorption kinetics tests was similar to the above adsorption isotherms experiments. The supernatant was collected every 2h for UV determination after centrifugation at 3000 *g* for 5 min.

2.5 Selectivity experiments

Two proteins (BSA, Lys) with different isoelectric points (pI) and molecular weights (MW) were chosen as the reference proteins to investigate the selectivity of the prepared HMIMs. For the separated adsorptions, each protein solution with an initial concentration of 0.2 mg mL^{-1} was applied to bind with HMIMs and NIMs, respectively. The final concentrations of HHb, BSA and Lys were measured by a UV/Vis spectrophotometer at 406 and 280 nm, respectively.

2.6 QCM evaluation

A 9 MHz quartz crystal microbalance (QCM) was used to quantify the interactions between the target proteins and the HMIMs (or NIMs)

prepared. A self-constructed oscillator circuit powered by a 5 volts D.C. voltage regulator was used to resonate the piezoelectric crystal with frequency output monitored by a frequency counter (Heathkit model IM-4120). The quartz crystal was bonded to a plastic tube by silicone rubber to form a detection cell and only one side of the crystal was coated with MIP. The coating procedure of the QCM with HMIMs and NIMs was as the following: Firstly, 0.5 mg of polyvinylchloride (PVC) powder was dissolved in 1 ml tetrahydrofuran (THF), then 2 mg of HMIMs and NIMs microspheres were dispersed into above solution. Proper volume of the suspension fluid was placed onto the Ag-electrode surface of the QCM. After THF was evaporated at room temperature, a polymer coating was formed on the Ag-electrode. The total frequency shift due to the surface modification was controlled to be about 8.0×10^3 Hz. Before determination, the HMIMs-coated electrode was stabilized in 0.2 mL of Tris-HCl buffer (pH 7.0, 0.01M) for several minutes until the frequency (f_0) was stable. A series concentration of HHb standard solutions at different concentrations were then injected into the detection cell. The measurements were carried out in an oscillated buffer solution at room temperature. The frequency (f_i) of the HMIMs-coated electrode at different times was recorded. The frequency shift (Δf_i) was calculated as $\Delta f_i=f_i-f_0$. After measurement, the HMIMs-coated electrode was washed three times with 0.5 M NaCl and deionized water, respectively. Each

wash was lasted for 10 min. The regenerated QCM was then ready for reuse. The investigation of NIMs-coated electrode was performed as the same with HMIMs-coated electrode.

3. Results and Discussion

3.1 Synthesis and characterization of functionalized silica microspheres

According to previous report, functionalizing the surface of nano-silica particles with carboxyl groups was helpful for the formation of imprinting material for lysozyme by noncovalent interaction [26]. Based on this report, the surface of silica microspheres has been modified with amino group and carboxyl group successively. Firstly, amino group was introduced on the surface of silica microspheres through the interaction between the silica microspheres and APTMS. Then, the silica microspheres were further functionalized with vinyl and carboxyl groups though the reaction with maleic anhydride. Thus, the modified silica microspheres not only possess the amino and carboxyl group on the surface of silica microspheres to form the strong synergistic hydrogen bonds with target protein HHb, but also have the polymerizable double bonds which could react with the monomer and crosslinker during the

subsequent imprinting process to form the crosslinked polymer (Scheme 1).

In order to confirm if the amino and carboxyl groups have been introduced on the surface of silica microspheres, the infrared spectra and electron energy spectra of the bare silica microspheres and functionalized silica microspheres were investigated, respectively. As can be seen in Fig. 1, there are no both bands of N-H stretching vibration around 2900 cm^{-1} and C=O stretching vibration around 1700 cm^{-1} in silica microspheres (Fig. 1, line a), which means that there are no $-NH_2$ and C=O groups in the bare silica microspheres; whereas, an apparent N-H stretching vibration band at 2939 cm^{-1} and C-N stretching vibration band at 1575 cm^{-1} could be observed in the amino functionalized microspheres (Fig. 1, line b). It implies that the surface of silica microspheres has been successfully modified with amino group. Meanwhile, the bands of 1710 cm^{-1} and 1647 cm^{-1} in SiO_2-R-NH-COOH can be assigned as the stretching vibration band of C=O and C-O, respectively (Fig. 1, line c). In addition, the band of 1396 cm^{-1} is produced by the in-plane bending vibration of O-H group. These characteristic bands of -COOH suggest clearly that the carboxyl group was introduced successfully on the surface of the SiO_2-R-NH-COOH microspheres. It is noted that the band of 2942 cm^{-1} still exist in SiO_2-R-NH-COOH microspheres. This result indicates that there are still some naked $-NH_2$ in SiO_2-R-NH-COOH microspheres,

which can form the synergistic hydrogen bond reaction with the functional group of target protein.

<Fig. 1>

In order to further verify above results, the electron energy spectra of silica microspheres before and after the modification have been investigated. As can be seen in Fig. 2, the C peak and N peak appear apparently in the spectrum of the functionalized microspheres (Fig. 2B), while do not show in the spectrum of silica microspheres (Fig. 2A), which further confirmed that the amino and carboxyl groups have been successfully functionalized on the surface of SiO_2 microspheres.

<Fig. 2>

3.2 Synthesis and characterization of HHb-imprinted microspheres

With the functionalized silica microspheres as support, surface imprinting of HHb was generated in aqueous monomer solution as shown in scheme 1. The HMIMs were eventually obtained after the removal of the embedded template protein. The SEM images of HMIMs and NIM were shown in Fig. 3. A layer of polymer can be seen obviously on the surface of microspheres, especially for the HMIMs , which illustrated that the functionalized vinyl group has really reacted with the monomers and cross-linking during the polymerization. To further confirm the existence

of polymer on the surface of HMIMs and NIMs, a thermogravimetric analysis was performed. As can be seen from Fig. S1, the weight loss of both HMIMs and NIMs were higher than that of microspheres which had never taken part in the process of polymerization. The results indicated that the layers of polymer had been formed successfully during the process of preparing HMIMs and NIMs through the interaction between the functional group and the monomers and crosslinkers.

<Fig. 3>

3.3 Rebinding capacity and kinetics of HMIMs and NIMs

To study the adsorption isotherms, experiments were conducted with a series of HHb solution with concentration ranging from 10 to 500 μg mL^{-1}. As can be seen from Fig. 4, the rebinding capacities of the HMIMs and NIMs to HHb are quite different. Within the given concentration range, the binding amounts of HMIMs are much higher than that of NIMs, especially when the initial concentration of HHb was higher than 200 μg mL^{-1}. It is noted that the binding amount gap between the HMIMs and NIMs is small at low HHb concentrations. This is possibly attributed to that the nonspecific adsorption played a dominant role played a dominant role at low concentration of HHb while the specific adsorption was more apparent at high concentration of HHb [45]. The different binding amount

between HMIMs and NIMs certified the existence of the imprinting cavities on the surface of the HMIMs.

<Fig. 4>

The rebinding kinetics experiments were conducted with an initial HHb concentration of 200 μg mL^{-1}. As shown in Fig. 5, the HMIMs reached the maximum adsorption at 4 h, while the NIMs climbed slowly as the time went by, indicating that the HMIMs showed a faster rebinding rate than NIMs. What is more, the rebinding amount of HMIMs towards template protein is obviously higher than NIMs, which further confirmed that the spatial integrity of the recognition sites has been formed on the surface of HMIMs during the imprinting process. The faster rebinding rate and the higher rebinding amount of HMIMs are attributed to the existence of imprinting cavities on HMIMs. On the other hand, NIMs are lack of imprinting cavities for, thus the structures of the formed polymers are estimated not as loose as HMIMs, which brought about the low binding rate and capacity.

<Fig. 5>

3.4 Specificity and selectivity of HMIMs

To investigate the specificity and selectivity of HMIMs towards HHb,

two other proteins with different isoelectric points (pI) and molecular weights (MW) were chosen as references in the selectivity experiments. The pI and MW of those proteins are as follows: HHb (pI 7.2, MW 64.5 W), BSA (pI 4.7, MW 67 W), Lys (pI 11.1, MW 1.4 W). The adsorption capacities of HMIMs and NIMs to these proteins in pH 7.0 Tris-HCl buffer with a feed concentration of 200 μg mL^{-1} were shown in Fig. 6. The ratio of binding capacity of HMIMs to NIMs is defined as imprinting factor (IF). It can be seen from Fig. 6 that the HMIMs exhibit significant adsorption selectivity to HHb with the highest IF of 1.90, and show a specific rebinding amount of 98 mg g^{-1} to HHb, higher than that of BSA which has the similar molecular weight as HHb. The results are attributed to the intrinsic selectivity due to the recognition sites on the surface of HMIMs.

Meanwhile, it is also noticed that both of HMIMs and NIMs exhibit higher rebinding capacity towards Lys. This is possibly ascribed to that Lys molecule is so small (1.4 W) that it is easier to entrance into the polymer cavities, including specific imprinting cavities and non-specific cavities.

<Fig. 6>

3.5 Regeneration and Reproducibility

In order to test the reusability of HMIMs, the HHb adsorption-desorption procedures were repeated for 4 times with the same imprinted microspheres at room temperature. After each adsorption, the HMIMs and NIMs were washed by 0.5 M NaCl solution and deionized water until no UV absorption of HHb could be detected by a UV/Vis spectrophotometer at 406 nm. As shown in Fig. 7, the adsorbed amounts of HHb on HMIMs have hardly changed after four cycles of adsorption-desorption. These results indicate that the obtained HMIMs are easy to regenerate and can be reused for several times.

<Fig. 7>

3.6 QCM Evaluation

To further investigate the selective recognition property of HMIMs to target HHb, HMIMs and NIMs are used as the sensing coatings on the 9 MHz quartz crystal microbalance (QCM). The frequency responses of HMIMs-coated electrodes and NIMs-coated electrodes to various target proteins were shown in Fig. 8. And the representative time course of the frequency change (ΔF) of HMIMs-coated electrode and NIMs-coated electrode to HHb was shown in Fig. 8 (insert curve). As shown in Fig. 8 that the HMIMs-coated electrode showed a much bigger response to HHb (Fig. 8, solid square) than BSA (Fig. 8, solid cycle). The distinctly

different responses are ascribed to the stronger interaction between HMIMs and HHb. Meanwhile, the NIMs-coated electrode showed a quite small response to both HHb (Fig. 8, solid inverted triangle) and BSA (Fig. 8, solid triangle), which implies that there is very weak adsorption occurred between NIMs and the proteins. The selective response to HHb of HMIMs certified the existence of the specific binding sites at the surface of HMIMs. Thus, the HMIMs modified QCM can provide a convenient way for the fast sensing of HHb solution with high sensitivity. Since there is no recognition sites at the surface of NIMs, HHb and BSA showed similar rebinding curves on the NIMs coated QCM sensor.

<Fig. 8>

4. Conclusions

The hydrophilic molecularly imprinted microspheres (HMIMs) functionalized with amino and carboxyl groups have been synthesized successfully using HHb as template protein. The introduced amino and carboxylic groups on the surface of microspheres play an important role in the formation of recognition sites for template protein through the hydrogen bond and electrostatic force during copolymerization. Thus, the HMIMs obtained have shown the improved imprinting effect for the template protein. The results from the characterizations of adsorption

isotherms, dynamic binding as well as quartz crystal microbalance (QCM) indicate that the HMIMs prepared exhibit good selectivity to target protein HHb. Besides HHb, the functionalized microspheres are expected to be used to imprint other target proteins, thus, providing a universal way for the preparation of sensitive materials for recognizing proteins in aqueous media.

Acknowledge

This work is supported by the National Natural Science Foundation of China (21107018, 21477026), Science and Technology Key Project of Ministry of Education (212129), Natural Science Foundation of Guangdong Province (2014A030313525).

References

1. R. X. Gao, X. Kong, X. Wang, X. W. He, L. X. Chen, Y. K. Zhang, *J. Mater. Chem.*, 2011, **21**, 17863-17871.
2. Z. A. Lin, Z. W. Xia, J. N. Zheng, D. Zheng, L. Zhang, H. H. Yang, G. N. Chen, *J. Mater. Chem.* 2012, **22**, 17914-17922.
3. Z. W. Xia, Z. A. Lin, Y. Xiao, L. Wang, J. N. Zheng, H. H. Yang, G. N. Chen, *Biosens. Bioelectron.*, 2013, **47**, 120-126.
4. D. Y. Li, X. W. He, Y. Chen, W. Y. Li, Y. K. Zhang, *ACS Appl. Mater. Interf.*, 2013, **5**, 12609-12616.

5. J. P. Lai, L. Xie, H. Sun, F. Chen, *Anal. Bioanal. Chem.*, 2013, **405**, 4269-4275.
6. H. Sun, J. P. Lai, Y. S. Fung, *J. Chromatogr. A*, 2014, **1358**, 303-308.
7. X. J. Li, B. L. Zhang, W. Li, X. F. Lei, X. L. Fan, L. Tian, H. P. Zhang, Q. Y. Zhang, *Biosens. Bioelectron.*, 2014, **51**, 261-267.
8. Y. T. Liu, Y. X. Gu, M. L. Li, Y. Wei, *New J. Chem.*, 2014, **38**, 6064-6072.
9. S. G. Hu, L. Li, X. W. He, *J. Chromatogr. A*, 2005, **1062**, 31-37.
10. X. H. Gu, R. Xu, G. L. Yuan, H. Lu, B. R. Gu, H. P. Xie, *Anal. Chim. Acta,* 2010, **675**, 64-70.
11. F. F. Chen, X. Y. Xie, Y. P. Shi, *Talanta*, 2013, **115**, 482-489.
12. J. P. Lai, R. Niessner, D. Knopp, *Anal. Chim. Acta*, 2004, 522, 137-144.
13. J. R. Qu, J. J. Zhang, Y. F. Gao, H. Yang, *Food Chem.*, 2012, **135**, 1148-1156.
14. J. Zhan, G. Z. Fang, Z. Yan, M. F. Pan, C. C. Liu, S. Wang, *Anal. Bioanal. Chem.*, 2013, **405**, 6353-6363.
15. M. L. Yola, L. Uzun, N. Ozaltin, A. Denizli, *Talanta*, 2014, **120**, 318-324.
16. F. J. Ning, H. L. Peng, L. L. Dong, Z. Zhang, J. H. Li, L. X. Chen, H. Xiong, *J. Agr. Food Chem.*, 2014, **62**, 11138-11145.
17. Y. S. Ji, J. J. Yin, Z. G. Xu, C. D. Zhao, H. Y. Huang, H. X. Zhang, C.

M.Wang, *Anal. Bioanal. Chem.*, 2009, **395**, 1125-1133.

18. L. G. Chen, X. P. Zhang, Y. Xu, X. B. Du, X. Sun, L. Sun, H. Wang, Q. Zhao, A. M. Yu, H. Q. Zhang, L. Ding, *Anal. Chim. Acta*, 2010, **662**, 31-38.
19. X. B. Luo, Y. C. Zhan, Y. N. Huang, L. X. Yang, X. M. Tu, S. L. Luo, *J. Hazard. Mater.*, 2011, **187**, 274-282.
20. M. Zarejousheghani, M. Moder, H. Borsdorf, *Anal. Chim. Acta*, 2013, **798**, 48-55
21. M. Zarejousheghani, P. Fiedler, M. Moder, H. Borsdorf, *Talanta*, 2014, 129: 132-138.
22. J. Dong, H. T. Fan, D. P. Sui, L. C. Li, T. Sun, *Anal. Chim. Acta*, 2014, **822**, 69-77.
23. H. C. Chen, D. Y. Yuan, Y. Y. Li, M. J. Dong, Z. H. Chai, J. Kong, G. Q. Fu, *Anal. Chim. Acta*, 2013, **779**, 82-89.
24. Q. Q. Gai, F. Qu, Z. J. Liu, R. J. Dai, Y. K. Zhang, *J. Chromatogr. A*, 2010, 1217, 5035-5042.
25. H. C. Chen, J. Kong, D. Y. Yuan, G. Q. Fu, *Biosens. Bioelectron.*, 2014, **53**, 5-11.
26. G. Q. Fu, H. Y. He, Z. H. Chai, H. C. Chen, *Anal. Chem.* 2011, **83**, 1431–1436.
27. H. C. Chen, D. Y. Yuan, Y. Y. Li, M. J. Dong, Z. H. Chai, J. Kong, G. Q. Fu, *Anal. Chim. Acta*, 2013, 779, 82-89.

28. W. Zhang, X. W. He, Y. Chen, W. Y. Li, Y. K. Zhang, *Biosens. Bioelectron.*, 2012, **31**, 84-89.

29. Z. Zhang, J. H. Li, J. Q. Fu, L. X. Chen, *RSC Adv.*, 2014, **4**, 20677-20685.

30. X. F. Zhang, X. Z. Du, X. Huang, Z. P. Lv, *J. Am. Chem. Soc.*, 2013, **135**, 9248-9251.

31. R. X. Gao, L. L. Zhang, Y. Hao, X. H. Cui, Y. H. Tang, *RSC Adv.*, 2014, 4, 64514-64524.

32. D. Z. Zhou, T. Y. Guo, Y. Yang, Z. P. Zhang, *Sens. Actuat. B*, 2011, **153**, 96-102.

33. D. Dechtrirat, K. J. Jetzschmann, W. F. M. Stocklein, F. W. Scheller, N. Gajovic-Eichelmann, *Adv. Funct. Mater.*, 2012, **22**, 5231-5237.

34. N. Sankarakumar, Y. W. Tong, *RSC Adv.*, 2013, **3**, 1519-1527.

35. X. J. Li, B. L. Zhang, L. Tian, W. Li, T. J. Xin, H. P. Zhang, Q. Y. Zhang, *Sens. Actuat. B*, 2014, **196**, 265-271.

36. H. Nishino, C. S. Huang, K. J. Shea, *Angew. Chem.-Int. Ed.*, 2006, **45**, 2392-2396.

37. C. H. Lu, Y. Zhang, S. F. Tang, Z. B. Fang, H. H. Yang, X. Chen, G. N. Chen, *Biosens. Bioelectron.*, 2012, **31**, 439-444.

38. A. M. Bossi, P. S. Sharma, L. Montana, G. Zoccatelli, O. Laub, R. Levi, *Anal. Chem.*, 2012, **84**, 4036-4041.

39. Y. Q. Yang, X. W. He, Y. Z. Wang, W. Y. Li, Y. K. Zhang, *Biosens.*

Bioelectron., 2014, **54**, 266-272.

40. A. A. Ozcan, R. Say, A. Denizli, A. Ersoz, *Anal. Chem.*, 2006, **78**, 7253-7258.

41. Q. Luo, Z. Y. Dong, C. X. Hou, J. Q. Liu, *Chem. Commun.*, 2014, **50**, 9997-10007.

42. X. P. Jia, M. L. Xu, Y. Z. Wang, D. Ran, S. Yang, M. Zhang, *Analyst*, 2013, **138**, 651-658.

43. H. Y. He, G. Q. Fu, Y. Wang, Z. H. Chai, Y. Z. Jiang, Z. L. Chen, *Biosens. Bioelectron*. 2010, **26**, 760–765.

44. A. Mehdinia, S. Dadkhah, T. B. Kayyal, A. Jabbari, *J. Chromatogr. A*, 2014, **1364**, 12-19.

45. F. Bonini, S. Piletsky, A. P. F. Turner, A. Speghini, A. Bossi, *Biosens. Bioelectron.* 2007, **22**, 2322-2328.

Legends of Schemes, Figures

Scheme 1 The synthetic route of the functionalized silica microspheres and HHb-imprinted microspheres

Fig. 1 The infrared spectra of the bare silica microspheres and functionalized silica microspheres

Fig. 2 The electron energy spectra of silica microspheres and functionalized silica microspheres (A: SiO_2, B: SiO_2-R-NH-COOH).

Fig. 3 The Scanning electron microscope of (a) NIMs, (b) HMIMs

Fig. 4 Adsorption isotherms of HHb on HMIMs and NIMs (Adsorption condition: V=10 mL, m=20 mg, adsorption time 10 h, room temperature, pH 7.0)

Fig. 5 Dynamic binding curve of HHb on HMIMs and NIMs (Adsorption condition: V=10 mL, m=20 mg, C_0=0.2 mg mL^{-1}, room temperature, pH 7.0)

Fig. 6 Rebinding amounts of different proteins on HMIMs and NIMs (Adsorption condition: $C_{0,HHb}$=200 μg mL^{-1}, V=10 mL, mass of HMIMs and NIMs is 20 mg, adsorption time 4 h, room temperature, pH 7.0)

Fig. 7 The repeatable test of HMIMs and NIMs (Adsorption condition: $C_{0,HHb}$ = 200 μg mL^{-1}, V=10 mL, mass of HMIMs and NIMs is 20 mg,

adsorption time 4 h, room temperature, pH 7.0)

Fig. 8 The frequency responses of HMIMs-coated electrode and NIMs-coated electrode to target proteins

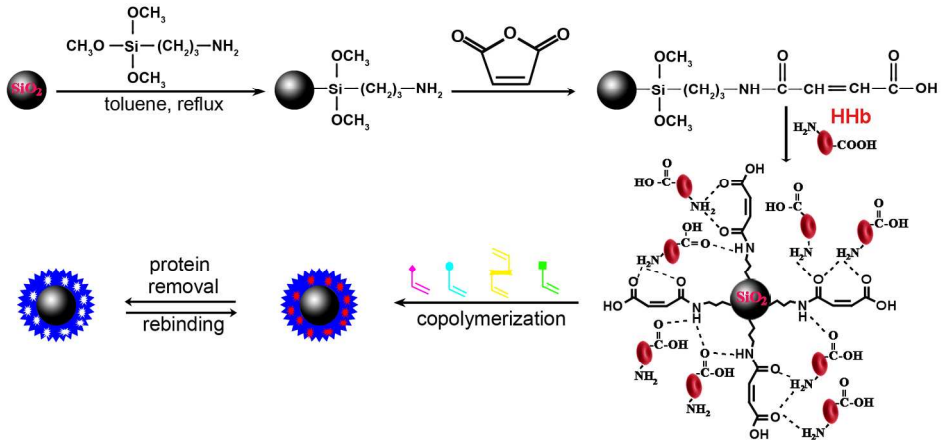

Scheme 1 The synthetic route of the functionalized silica microspheres and HHb-imprinted microspheres
186x84mm (300 x 300 DPI)

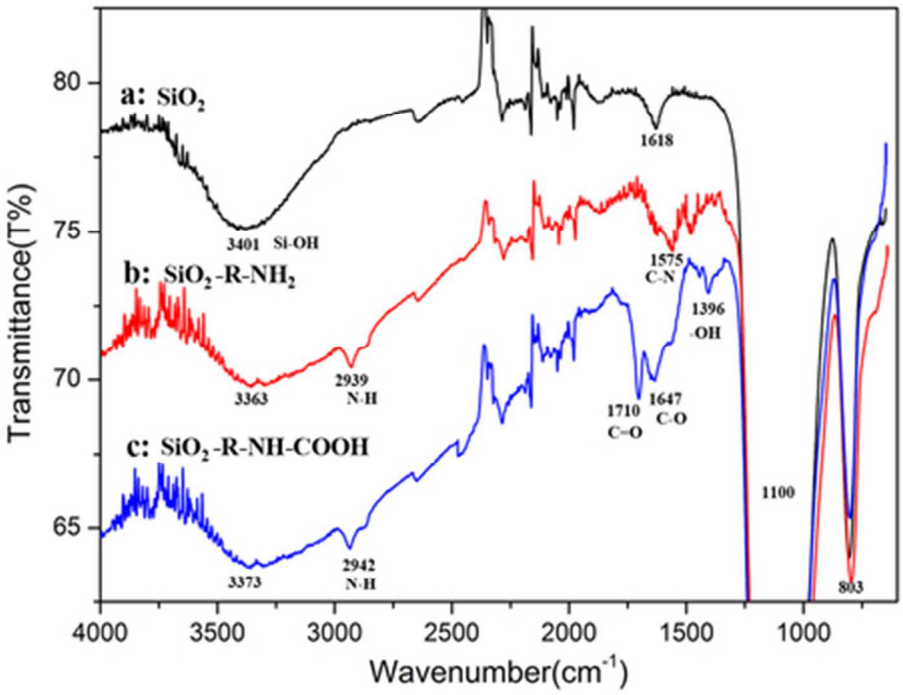

Fig. 1 The infrared spectra of the bare silica microspheres and functionalized silica microspheres
38x29mm (300 x 300 DPI)

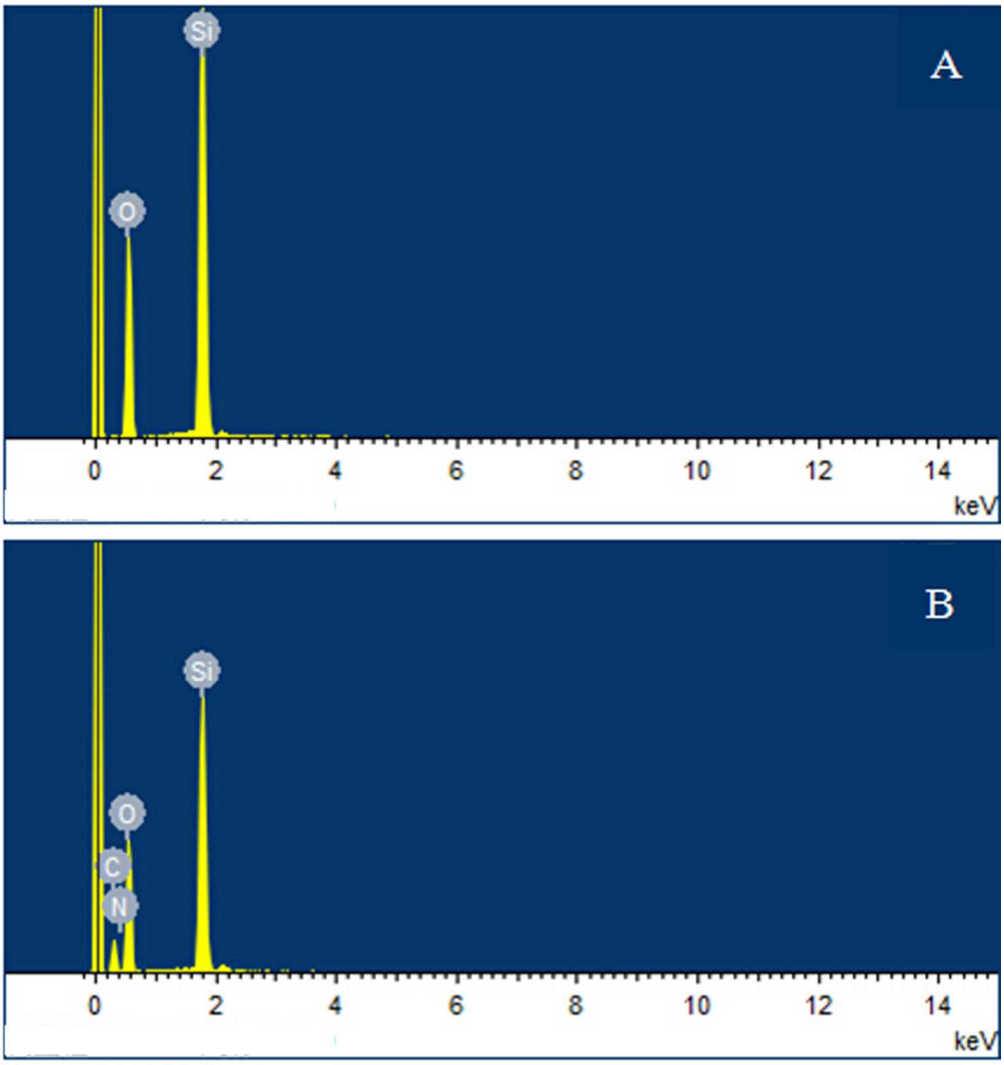

Fig. 2 The electron energy spectra of silica microspheres and functionalized silica microspheres (A: SiO2, B: SiO2-COOH)
113x120mm (300 x 300 DPI)

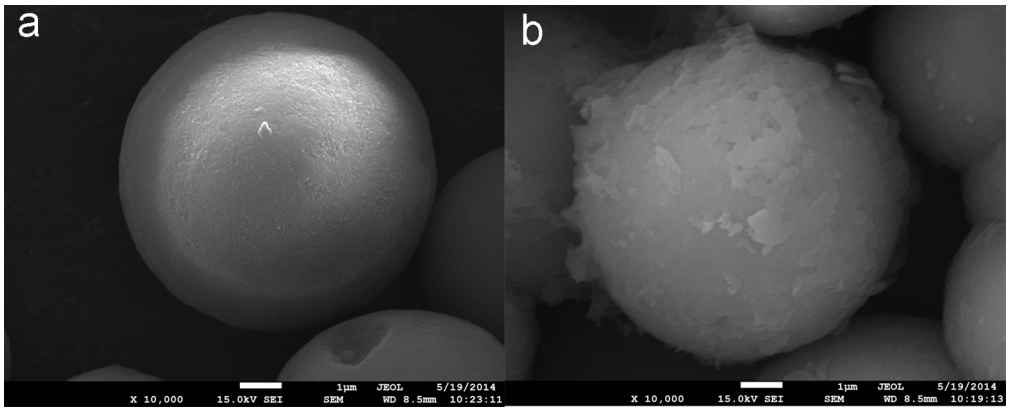

Fig. 3 The Scanning electron microscope of (a) NIMs, (b) HMIMs
146x58mm (300 x 300 DPI)

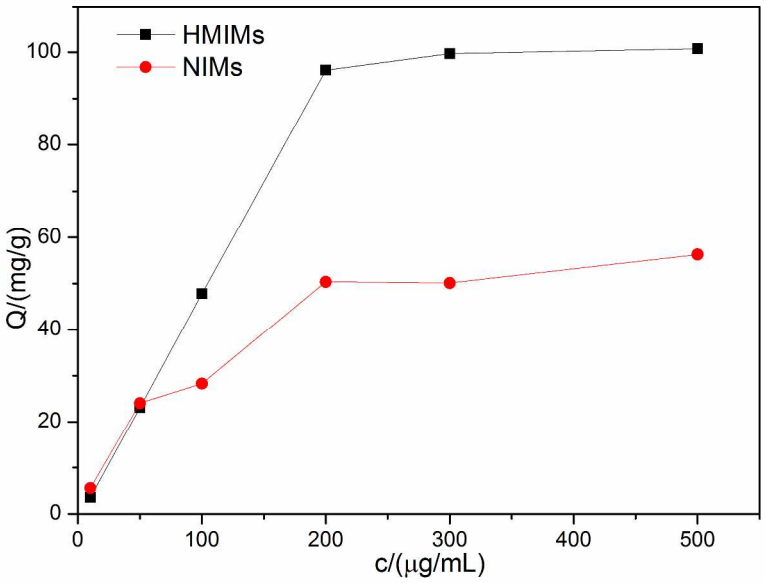

Fig. 4 Adsorption isotherms of HHb on HMIMs and NIMs (Adsorption condition: V=10 mL, m=20 mg, adsorption time 10 h, room temperature, pH 7.0)
296x209mm (300 x 300 DPI)

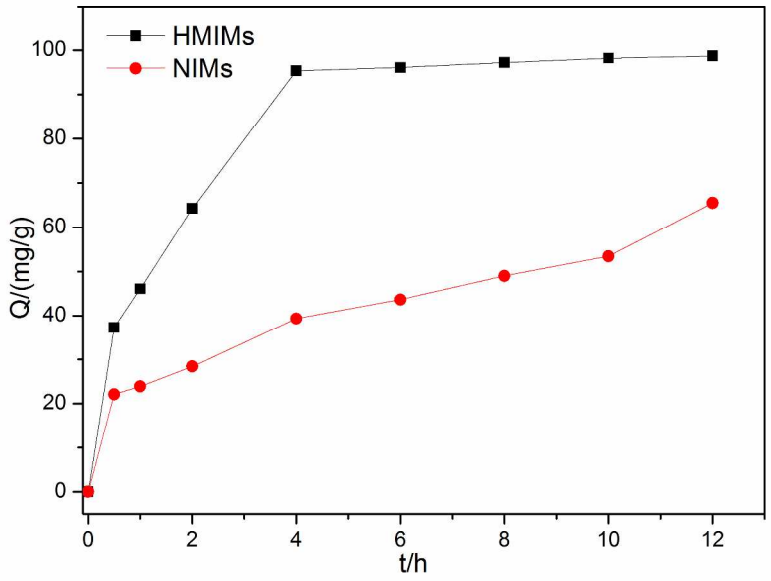

Fig. 5 Dynamic binding curve of HHb on HMIMs and NIMs (Adsorption condition: V=10 mL, m=20 mg, C0=0.2 mg mL-1, room temperature, pH 7.0)
296x209mm (300 x 300 DPI)

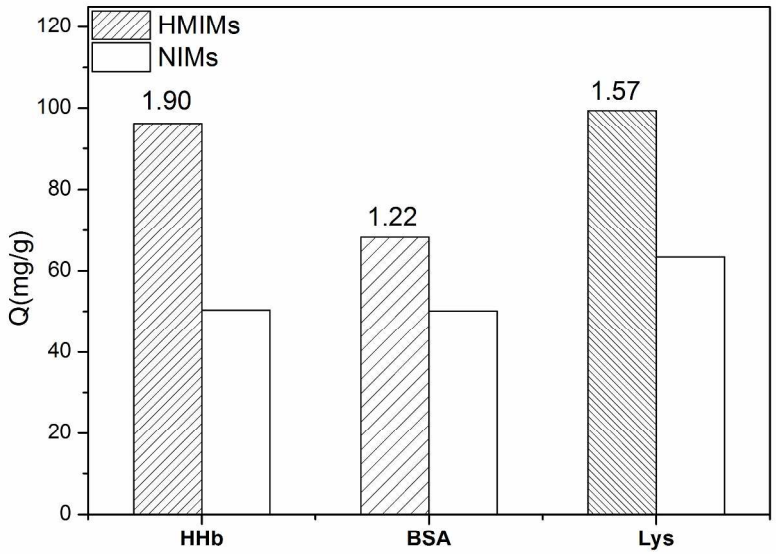

Fig. 6 Rebinding amounts of different proteins on HMIMs and NIMs (Adsorption condition: C0,HHb=200 μg mL-1, V=10 mL, mass of HMIMs and NIMs is 20 mg, adsorption time 4 h, room temperature, pH 7.0)
296x209mm (300 x 300 DPI)

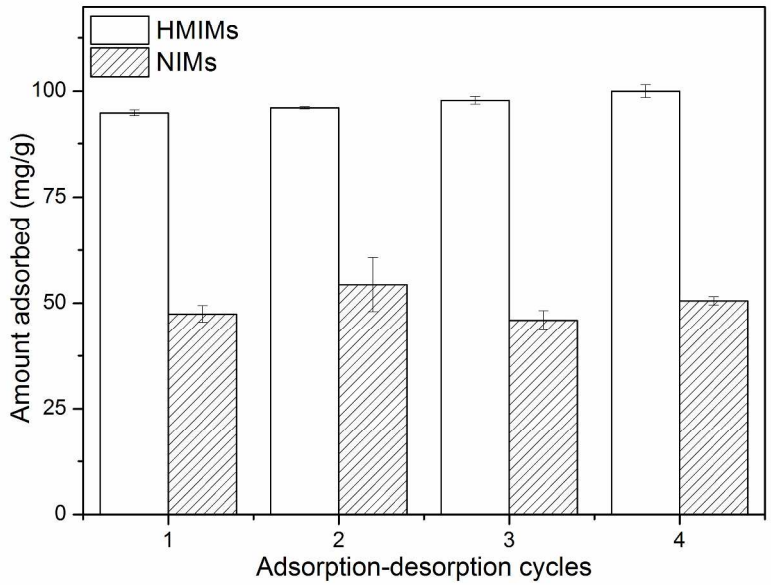

Fig. 7 The repeatable test of HMIMs and NIMs (Adsorption condition: C0,HHb = 200 μg mL-1, V=10 mL, mass of HMIMs and NIMs is 20 mg, adsorption time 4 h, room temperature, pH 7.0)
296x209mm (300 x 300 DPI)

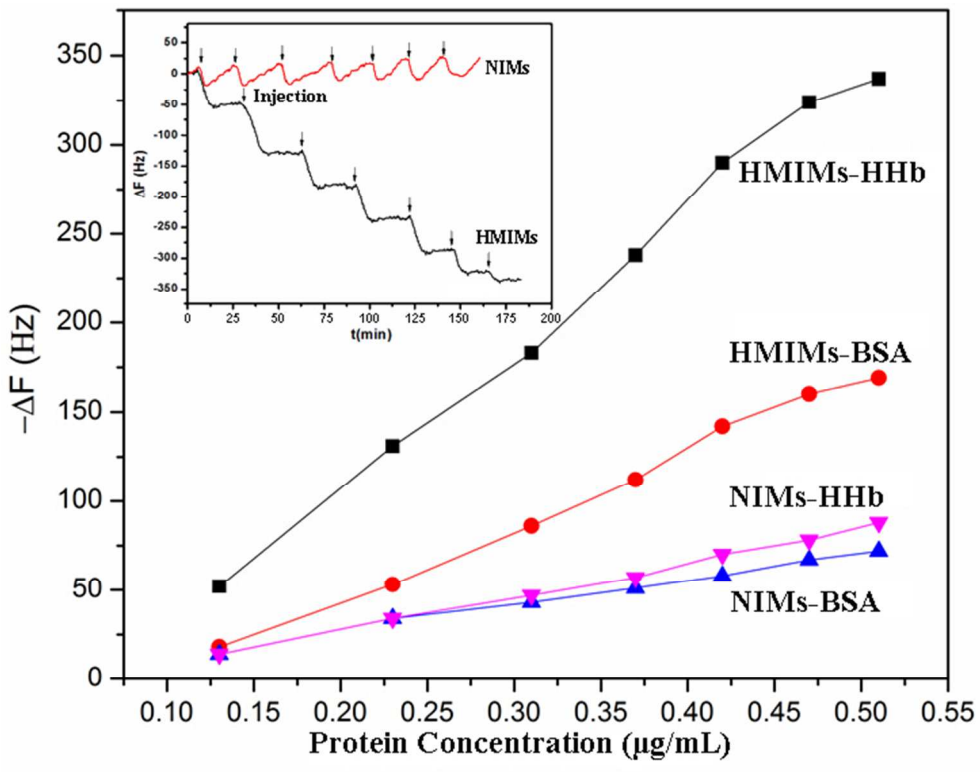

Fig. 8 The frequency responses of HMIMs-coated electrode and NIMs-coated electrode to target proteins
195x150mm (96 x 96 DPI)